Richwalski, S. M., Roth, F. (2008): Elastic and visco-elastic stress triggering in the South Iceland Seismic Zone due to large earthquakes since 1706. - Tectonophysics, 447, 1-4, 127-135

DOI: 10.1016/j.tecto.2006.06.009

# Elastic and visco-elastic stress triggering in the South Iceland Seismic Zone due to large earthquakes since 1706

Sandra M. Richwalski[1,2] and Frank Roth[2]

[1]Center for Disaster Management and Risk Reduction Technology (CEDIM), Karlsruhe, Germany
[2]GeoForschungsZentrum Potsdam, Potsdam, Germany

Corresponding author:
Sandra M. Richwalski, Telegrafenberg, 14473 Potsdam
E-mail: richw@gfz-potsdam.de
Fax: ++49 331 288 1204

**Abstract**

Damaging earthquakes in the South Iceland Seismic Zone (SISZ) occur fairly regularly and often as a series of events with a few days only between individual events. Tolerably reliable information on epicentre locations and mechanisms are available for 13 M ≥ 6 events between 1706 and 2000. For these events, we computed the co- and post-seismic stress fields, hereby approximating the SISZ by a mixed elastic/visco-elastic layered half-space. The horizontal shear stress and the Coulomb stress changes were analysed to detect possible trigger mechanisms, which may aid future earthquake mitigation efforts. We tested several criteria but must conclude that the start of an earthquake series in the SISZ cannot be explained by triggering through previous events. Inside an individual series, however, one may infer triggering. Our results are in contradiction with findings in other regions of the world. The reason might be related to the fact that the SISZ is not a mature fault zone, in which old faults are re-activated if a certain stress level threshold is passed. In addition, uncertainties in the model parameters as well as the neglect of horizontal variations in the model and of possible stress transfer due to volcanic activity further complicate the evaluation of our results and need to be taken into account in future studies.

***Keywords:*** SISZ, dislocations, modelling, shear stress, Coulomb stress change, rheology

## 1. Introduction

The probabilistic approach to determine seismic hazard assumes that earthquakes occur randomly in space and time. Contrary to this, several authors have found evidence that an event may trigger or prevent a subsequent one by changing the shear or Coulomb stress on the fault of this subsequent event (for an overview of the subject see e.g., Harris, 1998, Harris, 2000, or Freed, 2005). Hence, stochastically speaking, the likelihood of the next event is conditionally increased or decreased. In the South Iceland seismic zone (SISZ) this was found to be true for the two large earthquakes in June 2000 (e.g., for co-seismic triggering: Árnadóttir et al., 2003 and 2004; for poro-elastic post-seismic triggering: Jónsson et al., 2003).

Stress triggering at first sight seems to provide the means to identify future regions of potential earthquake hazard. However, reports of successful identification of triggering are often made with hindsight and for regions where fault systems have evolved over millions of years, with evidence that many faults are very old and the stress regime is stable. Moreover, many studies concentrate either on few events (sometimes only two successive ones) or consider only small time spans (a few years), taking only the elastic (immediate) response into account. Our goal was to study a whole series of events and, taking the time delays into account, we considered the visco-elastic post-seismic response important in the SISZ. Similar studies that span nearly or more than a century were published by Pollitz et al. (2003, 2004).

The SISZ is a 70 to 80 km long and 10 to 15 km wide zone taking up the transform motion forced upon Southern Iceland by the opening of two offset branches of the mid-Atlantic ridge (Figure1). The western branch continues on land as the Reykjanes Peninsula oblique rift zone. West of the SISZ lies the Western Volcanic Zone (WVZ) and east of it the Eastern Volcanic Zone (EVZ). There is no clear expression of an actual E-W trending transform fault and the SISZ is at an oblique angle with the neighbouring ridges. Damaging earthquakes (i.e. Ms ≥ 6, Figure 1) in the SISZ occur fairly regularly at intervals of several decades (Einarsson et al., 1981) and often as a series of events with time lags of generally only a few days between them. Generally, the first event in a series is the most eastward one, the subsequent events occur farther and farther west in the SISZ. All earthquakes occur as N-S oriented right-lateral strike-slip events.

Although the knowledge about the past events is far from complete (only the last three major events have been recorded instrumentally), the regularities observed so far, i.e., multiplicity of

events (sub-series), east-west migration of events belonging to one sub-series, and average recurrence time of sub-series, suggest a triggering mechanism. It seems obvious to assume that stress build-up by plate motion as well as stress changes caused by volcanic eruptions and seismic events, but also lateral inhomogeneities and the variation in crustal thickness determine the magnitude, location, and time of the impending event.

Therefore, Roth (2004) modelled the temporal evolution of the shear stress field by superimposing the background stress field caused by rift opening and the stress field changes induced by 13 events from 1706 to 2000. He applied an elastic half-space model and concluded that the respective pre-seismic shear stress levels at the location of the impending events were generally high enough for triggering (higher than the impending stress drop) and fairly stable, also when the size of the rupture planes was varied. Inside a sub-series, a mainshock-aftershock pattern became apparent. Roth (2004) explained inconsistencies by the incomplete knowledge about the events: slight E-W shifting of rupture planes might change the modelled pre-stress levels significantly in areas of inhomogeneous stress distributions. Due to the model being elastic, no post-seismic relaxation processes could be taken into account. These processes however have a significant influence on the stress distribution.

Encouraged by the results of Árnadóttir et al. (2003, 2004) and Jónsson et al. (2003) for the two large events in 2000 and by the findings of Roth (2004) we tried to find evidence for stress triggering for all or at least most of the 13 large events which occurred in the SISZ since 1706. We refined Roth's model by using a layered halfspace, in which the lower crust and mantle were considered to be visco-elastic. In addition to the steady stress increase of the stress field due to plate motion and seismic events, stress changes caused by relaxation were taken into account. Furthermore, we evaluated not only shear stress but also Coulomb stress changes along each rupture at 5 km depth.

## 2. Modelling method

Based on dislocation theory, Wang et al. (2003) developed software for computing the elastic deformation, strain, and stress field produced by slip on a surface in a layered half-space model. The software was then extended to allow for modelling a mixed elastic/visco-elastic layered half-space model (Lorenzo-Martín et al., 2002; Wang et al., 2006). This visco-elastic-gravitational extension can be used to model post-seismic creep processes. The software is composed of two parts, the first is called PSGRN and computes the Green's functions of the three fundamental double-couple point sources at pre-defined depths; PSCMP finalizes the output by linear combination of discrete sources on the fault plane(s). Slip on the rupture surface can be chosen non-uniformly. Geographical coordinates can be used for input and output, but all internal computations are carried out in model coordinates.

## 3. Model

Precise information about historical earthquakes is difficult to obtain for the time span considered in this study. Therefore, we tried to combine information from different authors consistently (Table 1).

For epicentral locations and width of the fault planes we followed Einarsson (pers. comm., 2004), who conducted field campaigns for mapping the surface expression of faults in the SISZ. He found evidence of a discrepancy between the published and actual locations of some faults, the former ones based mainly on isoseismal maps. He also estimated the increasing width (i.e. the vertical extent) of the rupture zone (from the surface down to the brittle-ductile transition) from the maximum depths of hypocentres published by Stefánsson et al. (1993). This width increases from 6 km in the western to 13 km in the eastern part of the SISZ. No information on the total length of the

ruptures was provided by Einarsson; therefore the values of Roth (2004; based on scaling relations) were taken. Since fault plane solutions are available only for the two events in 2000 (Dziewonski et al., 2001), all events are modelled as vertical N-S oriented right-lateral strike-slip events.

Crustal velocities of the model are shown in Figure 2 for S- and P-waves (Stefánsson et al., 1993), which are input variables for the computations. The transition from upper to lower crust is fixed at 6km, while that from lower crust to mantle is fixed at 24.5 km (an average value for the SISZ according to Menke, 1999). Viscosity estimates for the lower crust and mantle in Iceland range from $10^{18}$ Pas to $5 \cdot 10^{19}$ Pas (Jónsson et al., 2003, and references therein). We tested two values, $10^{18}$ Pas (corresponds to a relaxation time of less than 10 years) and $10^{19}$ Pas. In the latter case the visco-elastic material reacts much slower and stress changes can be expected decades after the event. We used the latter viscosity in the final model, because it better fits to the recurrence interval of seismic energy release.

Based on the damage caused by the instrumentally recorded 1912 event, Einarsson (pers. comm., 2004) estimated surface magnitudes for the historical events. Using Kanamori (1977) he derived scalar moment values based on the assumption that the shear modulus ranges between 30-60 GPa in crust and upper mantle. Hence, we computed the co-seismic slip $U_0$ using a constant shear modulus in this range. Roth (2004) used 39 GPa, which is rather high compared to values found in the literature (e.g., Stefánsson et al., 1993: 34 GPa; Pedersen et al., 2003: 30 GPa), but used in the absence of further constraints. Note, that for the crustal model of Stefánsson et al. (1993) a shear modulus of 39 GPa is reached at a depth of about 6 km, but values in the upper crust are much lower (down to 11 GPa).

The stress field computed for our model was evaluated at 101 grid points in N–S and at 141 grid points in E–W direction, which corresponds to a grid spacing of about 1x1 km.

## 4. Results

### *4.1 Horizontal shear stresses*

To study the temporal variation of the shear stress field in the SISZ we evaluated the E-W component of the stress tensor in a vertical plane. The procedure requires also a starting or background field, caused for the case at hand by tectonic loading and events before 1706. Then successively, we summed up the stress field produced by further tectonic loading in the inter-seismic times and superimposed the elastic and visco-elastic stress field changes caused by the individual events. We evaluated the horizontal shear stresses at a depth of 5 km, which can be used to represent an average hypocentral depth throughout the SISZ. We computed the average shear stress along the rupture before and after each event.

For the background field we followed the idea of Roth (2004), who had accounted in his elastic half-space modelling for the stress fields of the rifts neighbouring the SISZ. Due to the rift opening contribution being small, we assumed that an equivalent background model produced by a pure vertical strike-slip event in E–W direction would suffice. Since we have scarce knowledge on earthquakes before 1706, we need to make assumptions about the level of shear stress and its lateral variation. Regarding the latter, we refrained from assigning to the background field any additional lateral variation. Regarding the level, we assumed that the event of 14 August 1784 was the largest one for a long time-span. Furthermore, we assumed that only tectonic loading and no co- or post-seismic shear stress increase due to the events of 1706, 1732, and 1734 was responsible for building up the shear stress that was finally released on 14 August 1784. This assumption is justified because of the distant location of the ruptures. Given the estimated slip of 4.1m and provided that the plate motion rate of 1.9 cm/year was valid also then, 215 years are needed to build up the stress released by the event of 14 August 1784. Having now a value for the yearly stress built-up by plate motion, we constructed the stress field in 1706 (Figure 3).

Figure 3 shows the evolution of the shear stress field. As described above, we successively

accounted for the co- and post-seismic contribution of the individual events and a background stress field centred at 64.0° N. Clearly, the field in 1706 is too homogeneous. Roth (2004) considered the time up to and including 1784 as a tuning phase. From that time on we find a balanced distribution between areas of positive and negative stress. Events with magnitudes below M6 also modify the stress in the SISZ, but due to their impact on the stress change being small they are not considered in this study. Due to the parallel alignment of the ruptures and the consequential similarity of their stress patterns (location of lobes) the horizontal shear stress generally increases in E-W direction over time (increase of red areas), while in N-S direction it decreases (blue). Optically, the visco-elastic relaxation tends to smooth out the distribution of stresses such that small patches of low stress in high stress areas (and vice versa) vanish with time.

Figure 4 shows the averaged pre- and post-seismic shear stress levels at each rupture, both without (Figure 4a) and with (Figures 4b) postseismic relaxation. The stress values were interpolated between neighbouring grid points in E-W direction if necessary and then averaged along the rupture. Each panel is scaled to the maximum of the average pre- or post-seismic stresses along the individual rupture (Table 2). Since the time span between events inside a sub-series is small, the pre-seismic stress level is only evaluated before the first event in the sub-series. This leads to a total of 19 points in time, at which the stress is evaluated for each rupture location. However, we do not show the values connected to times after the specified event has happened. Figure 4c clarifies the connection between index number and point in time.

The maximum of the average pre- or post-seismic stresses is generally higher for the models which include co- and post-seismic stress changes than if co-seismic stress changes are considered only (Table 2). The shear stress reaches this maximum in only 6 out of the 12 cases (earthquakes of 1732, 1734, 1784a, 1896a, 1896c, and 1986e) before the subsequent event in the case of regarding only co-seismic stress changes (Figure 4a). Including also post-seismic changes (Figure 4b) increases the ratio to 7 out of 12 (1732, 1734, 1784a, 1896a, 1896c, 1986e, and 2000b). However, this means that for both cases the horizontal shear stress has already reached its maximum well before the event in nearly 50% of the cases (Table 3). Therefore, triggering should have occurred earlier in time, i.e. by the time of the first shear stress maximum.

### *4.2 Coulomb stress changes*

Moreover, we investigated whether the application of the Coulomb failure stress criterion explains stress triggering better than the analysis of the horizontal shear stress alone. Therefore, we computed the Coulomb stress changes (King et al., 1994) at 5 km depth on N-S oriented strike slip faults. We used a coefficient of friction of 0.75 (Árnadóttir et al., 2003) and a Skempton parameter of 0.5. The latter relates the change in pore pressure under drained conditions to that of confining pressure under undrained ones (Rice and Cleary, 1976). We evaluated what percentage of the total rupture trace showed a positive Coulomb stress change or even values above 0.01 MPa, a value generally considered the threshold for Coulomb triggering (see e.g. Reasenberg and Simpson, 1992; Hardebeck et al., 1998, Harris, 1998, and references therein). Inter-seismic stress changes, i.e. plate tectonics, were not considered in this analysis.

Figure 5 displays the Coulomb stress changes (ΔCFS) evaluated along each rupture (starting with the event of 1732). The ΔCFS caused by each previous event is plotted individually (bars in Fig. 5). We first checked whether the event under investigation was triggered by its preceding event. We are aware that asperity models may require relatively small patches of high stress. But since we do not know anything about the slip distribution on the rupture surfaces of the historical events, we require that at least 50% of the future rupture plane must show positive ΔCFS or a value above the usually assumed trigger threshold of 0.01 MPa. Then (Figure 5, Table 4), in 9 out of the 12 cases the ΔCFS was positive on at least 50 % of the rupture plane of the coming event (1732, 1734, 1784b, 1896a, 1896c, 1896d, 1896e, 1912 and 2000b), but only in 6 of the cases (1734, 1784b, 1896a, 1896c, 1896e and 2000b) was it above the threshold of 0.01 MPa. The only positive

finding is a correlation in so-called sub-series. Here, the events following the first event can be regarded as being triggered by ΔCFS in 6 out of 7 cases (1734, 1784b, 1896c, 1896d, 1896e and 2000b); the 1896d event shows on 50 % of the rupture plane positive Coulomb stress, but less than 50 % is above 0.01 MPa. In summary, for the sub-series we have found a mainshock-aftershock triggering pattern.

To complete the analysis, we considered delays as well. In the SISZ large events often occur as pairs or small clusters during the same day and within a time-span of up to 18.5 months (Sept. 1732 and March 1734; Aug. 14 and 16, 1784; Aug. 26, 28, Sept. 5 (2 events) & Sept. 6, 1896; June 17 and 21, 2000). If we neglect the events in these sub-series, we obtain a recurrence interval of 59 years for large events (series). If we investigate the delay of events by a preceding stress decrease in our Coulomb stress change analysis, we find - as far as 1st events of sub-series are considered - that the events in 1896a and 2000a are delayed by 53 and 29 years, respectively (Table 5). Even though the stress transfer in the two cases is not negative, it is at least low from 1912 to 2000a. However, the stress transfer is high from 1784 to 1896a, where it should be low, and is low from 1896 to 1912, where it should be high. We have summarized the results in Table 5.

Last but not least, as already found in the analysis of horizontal shear stress, the defined threshold for triggering was often already exceeded by events occurring before the preceding event. A linear increase or nearly constant level of ΔCFS before the preceding event can not be observed in Fig. 5. Rather, small and large ΔCFS values are distributed more or less randomly, indicating that most events should have been triggered already long before they actually happened.

## 5. Discussion

Computing horizontal shear stresses and Coulomb stress changes in the SISZ did not lead to definite conclusions regarding the timing and location of the impending event. Uncertainties in the model parameters (e.g. location of the historical events, rupture history, viscosity, knowledge about events prior to 1706, i.e. background stress field) as well as the simple approach used (e.g. 1D crustal structure, disregard of stress transfer due to volcanic activity) complicate the evaluation of the results. Generally, the modelling showed that it was not possible to constrain the stress field such that the impending event can only occur at its known location. There are always large areas in which stress levels seem to be high enough to trigger an event (Figure 3).

In view of the uncertainty of all input parameters, the results presented in Figure 3 should not be interpreted in an absolute sense. The magnitude of stress depends on e.g. the slip on the rupture surface, the shear modulus, and the viscosity. Without calibration of the modelling results with measured values, only the distribution of stresses should be considered. Additionally, this distribution is subject to uncertainties in the location of the events. As an example, we tested the influence of the choice of the viscosity value in the lower crust and mantle on our results. We repeated the calculations (which had been done for $10^{19}$ Pas) using $10^{18}$ Pas as well as $5 \cdot 10^{19}$ Pas. With the exception of the two events in 2000, the stress pattern given by the stress increase and decrease over time is very similar for the three different viscosity values and seems to have therefore little influence on possible triggering.

We conducted a detailed analysis of the modelling results only at the rupture locations shown in Table 1. The modelling of the temporal evolution of the horizontal shear stress field showed that regarding shear stress levels the maximum is only reached in 50% of the cases immediately before the event. Regarding Coulomb stress changes the following conclusions can be drawn: tectonic loading is certainly necessary as a precondition for single and first events of sub-series to occur. Subsequent events of such a sub-series might be regarded as being triggered by preceding events inside their sub-series. However, the spatial distribution of the events can again not be explained by our modelling. The observed migration of subsequent events towards the west might be correlated with the thinning of the crust towards the west. Additional 2D modelling might allow this hypothesis to be tested. Regarding interaction between earthquake and volcanic activity,

Gudmundsson and Saemundsson (1980) statistically analysed 82 eruptions and 44 seismic events for mutual influence and found a weak but significant relationship: volcanic activity precedes seismic activity. They argue that triggering might be possible, but they rather postulate a common cause, namely plate motion, which agrees with our findings that single and first events of sub-series cannot be explained by triggering through previous earthquakes.

Certainly, having better and more detailed information about previous events and subsurface parameters will lead to better modelling results. However, the SISZ cannot be considered a region with mature faults, which rupture with a certain recurrence interval. Furthermore, events in the SISZ appear parallel to each other. Successful Coulomb stress change reports come mainly from areas with one mature main fault running right through (e.g. North-Anatolian Fault Zone: Lorenzo-Martín et al. (2006); San Andreas Fault Zone), while secondary faults branch off or run only partly in parallel.

## 6. Conclusions

We can state that large events in the SISZ are presumably not triggered by preceding events but could rather occur randomly with the stress provided essentially by plate tectonics. Concerning the sub-series, our analysis indicates that when a large event strikes after a period of many years of relative quiescence, another large event is likely to occur during the ensuing few days or months.

Often the determination of Coulomb stress changes is used to calculate time-dependent probabilities of the occurrence of earthquakes, i.e. areas of positive ΔCFS are associated with an advance of future activity. For the SISZ, however, given the uncertainties in the input parameters (e.g. location of historical events) it seems presently unreasonable to determine temporal changes in the occurrence probability of future earthquakes.

Due to the peculiarities of the SISZ, namely, probable influence of volcanic activity (not accounted for in this study), and parallel alignment of ruptures (no mature fault system, i.e. no E-W trending through-going fault, but an en-echelon set of N-S trending faults), the application of stress transfer analysis techniques (horizontal shear stress and Coulomb stress changes) seems to be inappropriate for time intervals of more than a few days. However, the modelling approach presented here might be used elsewhere (provided input data quality is good) to identify future regions of potential earthquake hazard and to mitigate earthquake risk, as shown by Lorenzo-Martín et al. (2006).

## Acknowledgements

We acknowledge P. Einarsson and P. Halldórsson for making data available and giving insights on earthquake locations in the SISZ. We are grateful to R. Wang for providing the modelling software PRGRN/PSCMP. Figures were generated using GMT (Wessel and Smith, 1991). A. Schlums kindly revised our English. This research was carried out under EU-grant EVG1-CT-2002-00073 “PREPARED”.

## References

Árnadóttir, T., Jónsson, S., Pedersen, R., Gudmundsson, G.B., 2003. Coulomb stress changes in the South Iceland Seismic Zone due to two large earthquakes in June 2000. Geophys. Res. Lett., 30, 1205, doi: 10.1029/2002GL016495.

Árnadóttir, T, Geirsson, H., Einarsson, P., 2004. Coseismic stress changes and crustal deformation on the Reykjanes Peninsula due to triggered earthquakes on 17 June 2000. J. Geophys. Res., 109, B09307, doi: 10.1029/2004JB003130.

Einarsson, P., Björnsson, S., Foulger, G., 1981. Seismicity pattern in the South Iceland Seismic Zone. In: D.W. and Richards, P.G. (Eds.), Earthquake Prediction – An International Review,

Simpson. Maurice Ewing Series 4, AGU.
Dziewonski, A.M., Ekström, G., Maternoskaya, N.N., 2001. Centroid moment tensor solutions for April-June 2000. Phys. Earth Planet. In., 123, 1-14.
Freed, A. M., 2005. Earthquake triggering by static, dynamic, and postseismic stress transfer. Annu. Rev. Earth Pl. Sc., 33, 335-367.
Gudmundsson, G., Saemundsson, K., 1980. Statistical analysis of damaging earthquakes and volcanic eruptions in Iceland from 1550-1978. J. Geoph., 47, 99-109.
Hardebeck, J. L., Nazareth, J.J., Hauksson, E., 1998. The static stress change triggering model: Constraints from two southern California aftershock sequences. J. Geophys. Res., 103, 24427-24437.
Harris, R.A., 1998. Introduction to special section: Stress triggers, stress shadows, and implications for seismic hazard. J. Geophys. Res., 103 (B10), 24347-24358.
Harris, R. A., 2000. Earthquake stress triggers, stress shadows, and seismic hazard. Curr. Sci. India, 79 (9), 1215-1225.
Jónsson, S., Segall, P., Pedersen, R., Björnsson, G., 2003. Post-earthquake ground movements correlated to pore-pressure transients. Nature, 424, 179-183.
Kanamori, H, 1977. The energy release in great earthquakes. J. Geophys. Res., 62, 2981-2987.
King, G. C., Stein, R. S., Lin, J., 1994. Static stress changes and the triggering of earthquakes. B. Seism. Soc. Am., 84, 935-953.
Lorenzo-Martín, F., Wang, R., Roth, F., 2002. The effect of input parameters on visco-elastic models of crustal deformation. Física de la Tierra, 14, 33-54.
Lorenzo-Martín, F., Roth, F., Wang, R., 2006, Elastic and inelastic triggering of earthquakes in the North Anatolian Fault zone, Tectonophysics, in press.
Menke, W., 1999. Crustal isostasy indicates anomalous densities beneath Iceland. Geophys. Res. Lett., 26, 1215-1218.
Pedersen, R., Jónsson, J., Árnadóttir, T., Sigmundsson, F., Feigl, K.L., 2003. Fault slip distribution of two June $M_W$6.5 earthquakes in South Iceland estimated from joint inversion of InSAR and GPS measurements. Earth Planet. Sc. Lett., 213, 487-502.
Pollitz, F., Vergnolle, M., Calais, E., 2003. Fault interaction and stress triggering of twentieth century earthquakes in Mongolia. J. Geophys. Res., 108 (B10), 2503, doi: 10.1029/2002JB002375.
Pollitz, F., Bakun, W. H., Nyst, M., 2004. A physical model for strain accumulation in the San Francisco Bay region: Stress evolution since 1838. J. Geophys. Res., 109, B11408, doi: 10.1029/2004JB003003.
Reasenberg, P. A., Simpson, R. W., 1992. Response of regional seismicity to the static stress change produced by the Loma Prieta earthquake. Science, 255, 1687-1690.
Rice, J. R., Cleary, M. P., 1976. Some basic stress diffusion solutions for fluid saturated elastic porous media with compressible constituents. Rev. Geophys., 14, 227-241.
Roth, F., 2004. Stress changes modelled for the sequence of strong earthquakes in the South Iceland Seismic Zone since 1706. Pure Appl. Geophys., 161, 1305-1327.
Stefánsson, R., Böðvarsson, R., Slunga, R., Einarsson, P., Jakobsdóttir, S., Bungum, H., Gregersen, S., Havskov, J., Hjelme, J., Korhonen, H., 1993. Earthquake prediction research in the South Iceland Seismic Zone and the SIL project. B. Seism. Soc. Am., 83, 696-716.
Wang, R., Lorenzo-Martín, F., Roth, F., 2003. Computation of deformation induced by earthquakes in a multi-layered elastic crust – FORTRAN programs EDGRN/EDCMP. Comput. Geosci., 29, 195-207.
Wang, R., Lorenzo-Martín, F., Roth, F., 2006. PSGRN/PSCMP – a new code for calculating co- and post-seismic deformation, geoid and gravity changes based on the viscoelastic-gravitational dislocation theory. Comput. Geosci., 32 (4), 527-541.
Wessel, P., Smith, W.H.F., 1991. Free software helps map and display data. EOS, 72 (41), 441, 445-446.

**Figure captions**

Figure 1: The computational area including the South Iceland seismic zone (SISZ). Its location on Iceland is shown as inset. Also indicated are: Western (WVZ) and Eastern Volcanic Zone (EVZ); branches of the mid-Atlantic ridge (dashed lines); the position of the volcanoes Hengill, Hekla, and Katla (from west to east; triangles; positions from National Geophysical Data Center (NGDC) http://www.ngdc.noaa.gov and topographical maps). Ruptures (Roth, 2004; solid lines) and epicentres (Einarsson, pers. comm.; stars) of the 13 $M \geq 6$ earthquakes from 1706 to 2000 are also shown.

Figure 2: Model: P- and S-wave velocities were taken from Stefánsson et al. (1993). The viscosity in the lower crust and mantle is $10^{19}$ Pas (also values of $10^{18}$ Pas and $5 \cdot 10^{19}$ Pas were tested).

Figure 3: Temporal evolution of the horizontal shear stress field for the visco-elastic layered earth model. The background field is centred at 64.0° N. The location of the impending event(s) is indicated by bar(s). The '+' sign indicates that the stress field is shown including the co-seismic stress of the respective event. The '-' sign shows the stress field right before the event.

Figure 4: Comparison between elastic (Figure 4a) and visco-elastic (Figure 4b) modelling results for shear stress evolution, centring the background field at 64.0° N. The stress field was evaluated before and after each event. For events occurring within one year the inter-seismic time was assumed to be zero and post- and pre-event stress levels can be assumed to be equal. The connection between index number and point in time is shown in Figure 4c. For each rupture the maximum of the average shear stresses corresponding to 100% is shown in Table 2.

Figure 5: (a): Percentage of the rupture plane at 5 km depth of the indicated event that shows positive Coulomb stress (white) and values above the threshold of 0.01 MPa (black). The Coulomb stress change is evaluated for each event independently. The connection between index number and point in time is shown in Figure 5b.

**Table 1** Final model for the location and slip of the 13 events.

| Date | $M_S$ | Lat.ºN | Long.ºW | Length [km] | Width [km] | $M_0$ [$10^{19}$ Nm] | $U_0$ [m] |
|---|---|---|---|---|---|---|---|
| 20.04.1706 | 6.0 | 63.98 | 21.19 | 10 | 6 | 0.1 | 0.43 |
| 07.09.1732 | 6.7 | 63.97 | 20.04 | 22 | 13 | 1.4 | 1.26 |
| 21.03.1734 | 6.8 | 63.97 | 20.83 | 25 | 7 | 2.0 | 2.93 |
| 14.08.1784 | 7.1 | 63.97 | 20.48 | 35 | 10 | 5.6 | 4.10 |
| 16.08.1784 | 6.7 | 63.97 | 20.94 | 22 | 6 | 1.4 | 2.72 |
| 26.08.1896 | 6.9 | 63.99 | 20.13 | 28 | 12 | 2.8 | 2.14 |
| 27.08.1896 | 6.7 | 63.97 | 20.26 | 22 | 11 | 1.4 | 1.48 |
| 05.09.1896 | 6.0 | 63.98 | 20.99 | 10 | 6 | 0.1 | 0.43 |
| 05.09.1896 | 6.5 | 63.99 | 20.58 | 18 | 9 | 0.7 | 1.11 |
| 06.09.1896 | 6.0 | 63.98 | 21.19 | 10 | 6 | 0.1 | 0.43 |
| 06.05.1912 | 7.0 | 63.94 | 19.95 | 32 | 13 | 3.5 | 2.16 |
| 17.06.2000 | 6.5 | 63.97 | 20.36 | 16 | 10 | 0.7 | 1.12 |
| 21.06.2000 | 6.4 | 63.98 | 20.72 | 18 | 9 | 0.6 | 0.95 |

**Table 2** Maximum horizontal shear stresses averaged along rupture planes. Values correspond to 100% in Figures 4a (co-seismic) and 4b (co- and post-seismic).

| event | co-seismic [$10^6$ Pa] | co- and post-seismic [$10^6$ Pa] |
|---|---|---|
| 1732 | 2.1 | 2.1 |
| 1734 | 2.0 | 2.0 |
| 1784_a | 2.1 | 2.0 |
| 1784_b | 2.4 | 2.4 |
| 1896_a | 2.8 | 3.2 |
| 1896_b | 2.7 | 3.2 |
| 1896_c | 5.1 | 4.9 |
| 1896_d | 2.6 | 3.3 |
| 1896_e | 7.6 | 8.3 |
| 1912 | 2.0 | 2.5 |
| 2000_a | 3.1 | 3.2 |
| 2000_b | 3.1 | 3.2 |

Table 3 Evaluation of the stress level at the rupture plane of the triggered event (Fig. 5).

| | Elastic model | | Visco-elastic model | |
|---|---|---|---|---|
| Criterion | Success ratio | Events meeting the criterion | Success ratio | Events meeting the criterion |
| High, i.e. ≥50 % of maximum for that rupture | 10 / 12 | 1732, 1734, 1784a, b, 1896a, b, c, d, e, 2000b | 12 / 12 | all |
| Maximum since 1706 | 6 / 12 | 1732, 1734, 1784a, 1896a, c, e | 7 / 12 | 1732, 1734, 1784a, 1896a, c, e, 2000b |
| Maximum for 1st events only[a] | 3 / 5 | 1732, 1784a, 1896a | 3 / 5 | 1732, 1784a, 1896a |

[a] This refers to single events (1912) and 1st events of sub-series (1732, 1784a, 1896a, 2000a).

Table 4 Coulomb stress changes (for both the co-seismic and co- + post-seismic stress changes) at the rupture plane of the triggered event. Here, only pairs of triggering and triggered events are considered. The results of the elastic and the visco-elastic model differ but not essentially with respect to the criteria applied here.

| | ΔCFS > 0 MPa | | ΔCFS ≥ 0.01 MPa | |
|---|---|---|---|---|
| | Success ratio | Events meeting the criterion | Success ratio | Events meeting the criterion |
| At ≥50 % of the rupture plane | 9 / 12 | 1732, 1734, 1784b, 1896a, c, d, e, 1912, 2000b | 6 / 12 | 1734, 1784b, 1896a, c, e, 2000b |
| Maximum since 1706 | 2 / 12 | 1732, 1734 | 1 / 12 | 1734 |
| At ≥50 % of the rupture plane of 1st events[a] only | 3 / 5 | 1732, 1896a, 1912 | 1 / 5 | 1896a |
| At ≥50 % of the rupture plane inside clusters only | 6 / 7 | 1734, 1784b, 1896c, d, e, 2000b | 5 / 7 | 1734, 1784b, 1896c, e, 2000b |

[a] This refers to single events (1912) and 1st events of sub-series (1732, 1784a, 1896a, 2000a).

Table 5 Time delays (advances) for events due to stress decrease (increase) by Coulomb stress changes (for both the co-seismic and co- & post-seismic stress changes on different fractions of the rupture planes at 5 km depth). The results of the elastic and the visco-elastic model differ, but not essentially with respect to the criteria applied here.

| | Event | Timing | ΔCFS-criteria met hard → soft | | | |
|---|---|---|---|---|---|---|
| | | "-" early "+" late (in years) | ΔCFS > 0.01 MPa at ≥ 50 % | ΔCFS > 0 at ≥ 50 % | ΔCFS > 0.01 MPa at > 0 % | ΔCFS > 0 at > 0 % |
| 1st events only (average recurrence time 58.8 years) | 1732 | -32.4 | no | **yes** | no | yes |
| | 1784a | -6.9 | no | no | **yes** | yes |
| | 1912 | -43.2 | no | **yes** | no | yes |
| | | | | | | |
| | | | ΔCFS < -0.01 MPa at ≥ 50 % | ΔCFS < 0 at ≥ 50 % | ΔCFS < -0.01 MPa at > 0 % | ΔCFS < 0 at > 0 % |
| | 1896a | +53.2 | no | no | **yes** | yes |
| | 2000a | +29.3 | no | **yes** | yes | yes |

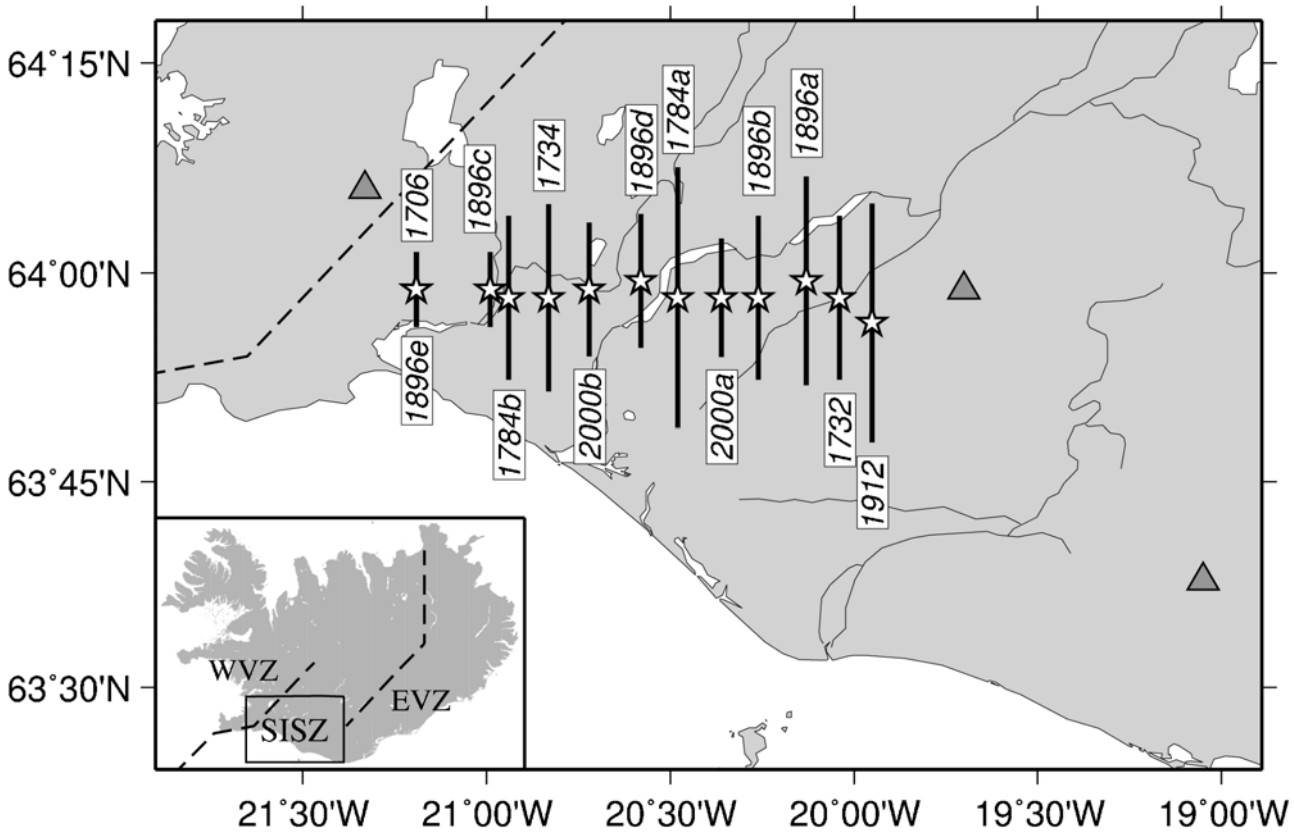
64˚15'N
64˚00'N
63˚45'N
63˚30'N
21˚30'W
21˚00'W
20˚30'W
20˚00'W
19˚30'W
19˚00'W
1706
1896c
1734
1896d
1784a
1896b
1896a
1896e
1784b
2000b
2000a
1732
1912
WVZ
EVZ
SISZ

Figure 1

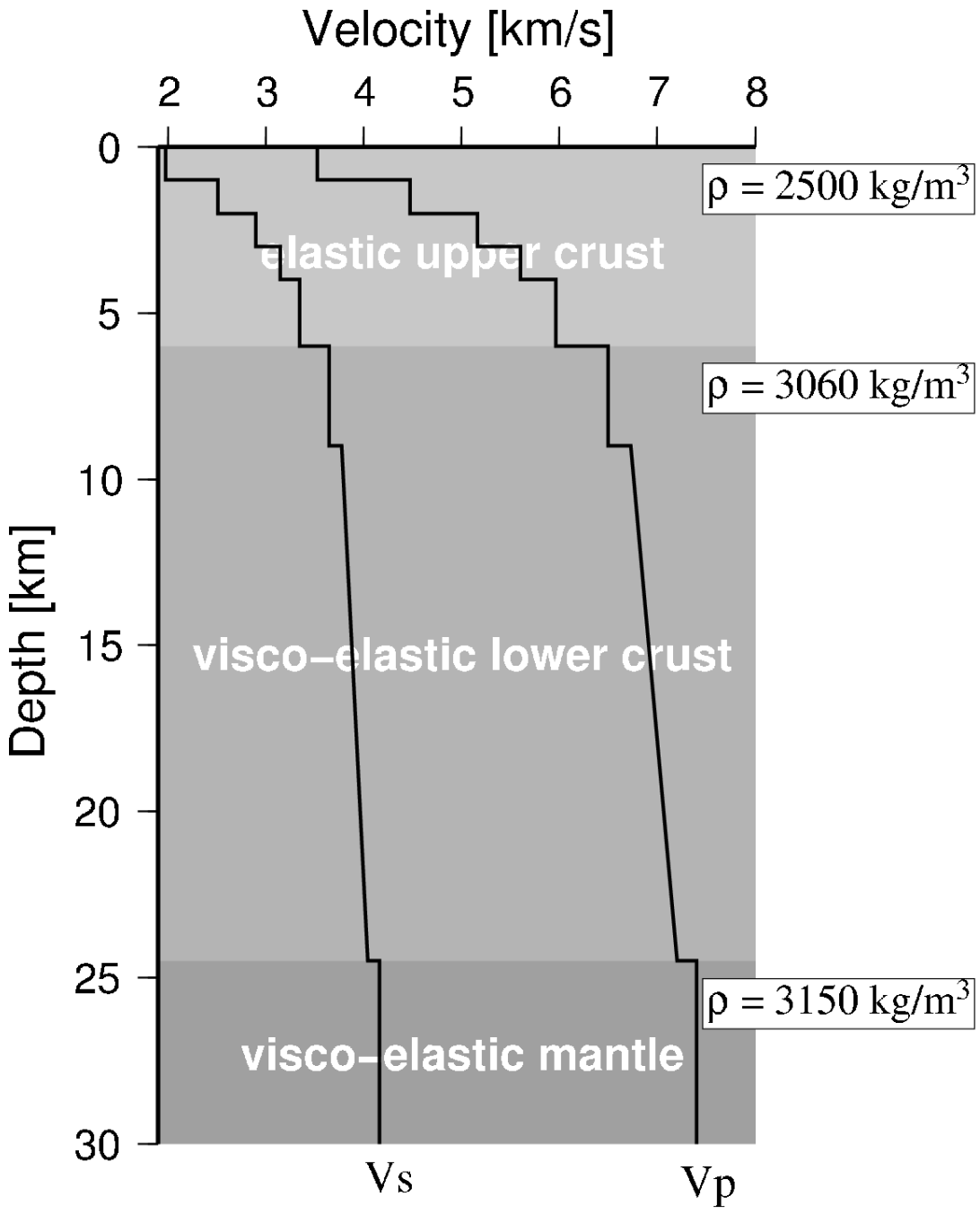
Velocity [km/s]
2
3
4
5
6
7
8
0
5
10
15
20
25
30
Depth [km]
ρ = 2500 kg/m3
elastic upper crust
ρ = 3060 kg/m3
visco−elastic lower crust
ρ = 3150 kg/m3
visco−elastic mantle
Vs
Vp

Figure 2

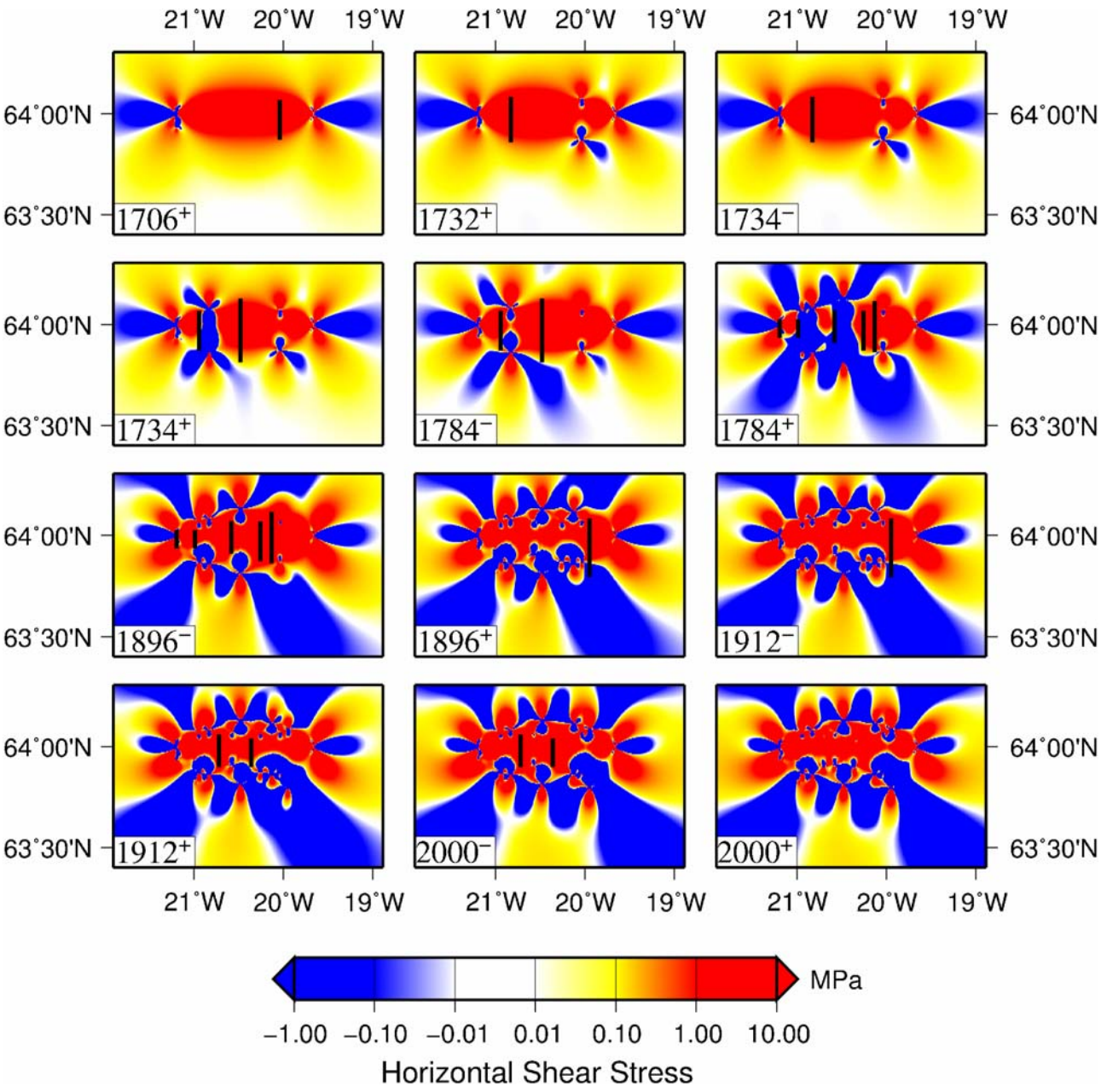
21°W
20°W
19°W
64°00'N
63°30'N
1706+
1732+
1734−
1734+
1784−
1784+
1896−
1896+
1912−
1912+
2000−
2000+
MPa
−1.00
−0.10
−0.01
0.01
0.10
1.00
10.00
Horizontal Shear Stress

Figure 3

Figure 4a

Figure 4b

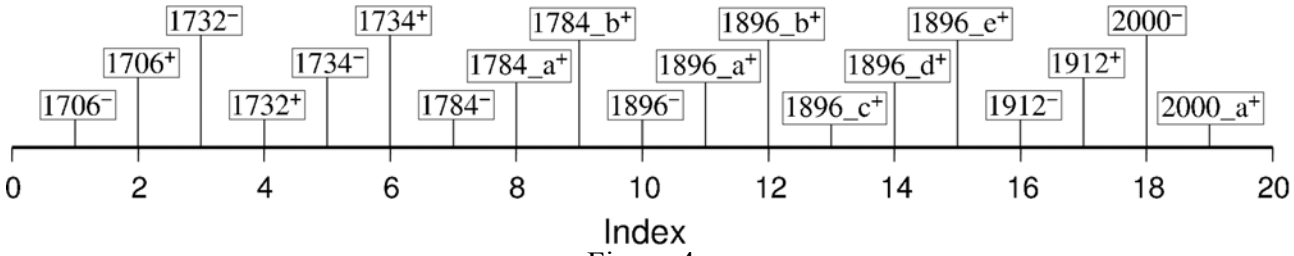

Figure 4c

Figure 5a



Figure 5b